Validation of TOPAS MC for modelling the efficiency of an extended-range coaxial p-type HPGe detector

Peer-reviewed author version

BRABANTS, Lowie; Lutter, Guillaume; Paepen, Jan; VANDOREN, Bram; RENIERS, Brigitte & SCHROEYERS, Wouter (2021) Validation of TOPAS MC for modelling the efficiency of an extended-range coaxial p-type HPGe detector. In: APPLIED RADIATION AND ISOTOPES, 173 (Art N° 109699).

DOI: 10.1016/j.apradiso.2021.109699
Handle: http://hdl.handle.net/1942/33851

Validation of TOPAS MC for modelling the efficiency of an extended-range coaxial p-type HPGe detector

Lowie Brabants[a], Guilaume Lutter[b], Jan Paepen[b], Bram Vandoren[c], Brigitte Reniers[a], Wouter Schroeyers[a*]

[a]Hasselt University, CMK, NuTeC, Nuclear Technology - Faculty of Engineering Technology, Agoralaan Building H, B- 3590 Diepenbeek, Belgium

[b]EC-JRC, European Commission, Joint Research Centre, Retieseweg 111, B-2440 Geel, Belgium

[c]Hasselt University, CERG, Faculty of Engineering Technology, Agoralaan Building H, B- 3590 Diepenbeek, Belgium

ABSTRACT

TOPAS MC software was used to model the efficiency of a coaxial p-type HPGe detector, type GX9023 from Canberra. The model was validated by comparing experimental efficiencies with efficiencies calculated by TOPAS MC simulations. Three different geometries of radionuclide sources, placed at different heights from the detector endcap, were used to validate the model. The imposed criteria of 5% relative difference was met for a range of radionuclides and gamma-ray energies. As a result, the created detector model with TOPAS MC was considered validated.

KEYWORDS

- Monte Carlo
- TOPAS MC
- High Purity Germanium Detector

1 INTRODUCTION

Gamma-ray spectrometry using High Purity Germanium (HPGe) detectors is one of the most common laboratory techniques for analysing samples containing gamma-ray emitting radionuclides. To achieve a good analytical performance for the HPGe detector, it is crucial that the detector is correctly calibrated with both an energy and an efficiency calibration. Both calibrations can be carried out with an experimental approach, by using reference materials or standard sources having a well-known composition, geometry and activity (Lutter et al., 2018). The calibration results can in turn be used to evaluate the radioactivity of unknown samples which have a similar composition and geometry as the used reference or standard. This also directly implies a practical limitation on the use of gamma-ray spectrometry where calibrations are performed with reference sources, as it is not always possible to obtain suitable materials that closely match the samples which need to be characterised (Saraiva et al., 2016).

To overcome these limitations, Monte Carlo (MC) simulations provide an alternative to reference sources as the simulated detector response of HPGe detectors can be used to derive the full-energy peak (FEP) efficiencies. Furthermore, the MC code can be used for a wide range of source geometries and material compositions, thus limiting the need for having a reference material for each sample encountered. Even when suitable reference or standard sources are available, MC models can be used as a supplemental computational technique to calculate correction factors to account for small differences between the reference source and the samples (such as small geometrical or chemical differences).

Because of the benefits of MC computational methods, extensive research has been carried out to simulate the detector response of HPGe detectors with a number of different codes. (Lutter et al., 2018) validated the EGSnrc Monte Carlo code to simulate the FEP efficiency by using the EGSnrc C++ class library called "egspp" developed by Kawrakow et al. (2017). This library was used to simulate photons. For simulating full radioactive decays, a decay generator was added to the code, resulting in a new code named "hpge3". This MC code has since its development been used for a wide range of HPGe related research at the Joint Research Centre (JRC) from dead-layer experiments to radiological characterizations of alkali activated concretes and ultra low-background measurements (Hult et al., 2019)(Croymans et al., 2017)(Hult et al.,

*Wouter Schroeyers; wouter.schroeyers@uhasselt.be; Hasselt University, Agoralaan – building H, 3590 Diepenbeek

2018). The EGSnrc models of the HPGe detectors are optimised for achieving an agreement within 5% relative difference between experimental efficiencies and simulated efficiencies (Hult et al., 2018).

(Khan et al., 2018) used the Geant4 Monte Carlo code to study the influence of endcap and dead-layer thickness on the FEP peak efficiency of a co-axial HPGe (ORTEC©) detector. The MC model was validated with experimental data of point sources placed at 150 mm from the endcap. The reported relative difference between the experimental and simulated FEP values were averaged for low energies and high energies and were respectively 3% and 5%, although higher deviations at energies above 898 keV were observed. In their research, no exact definition of the low and high energy range was formulated. (Cebastien Joel et al., 2018) developed a detector model for a broad-energy HPGe detector (Canberra type BE6530) with the Geant4 Monte Carlo code. The efficiency calibration of the detector was validated by comparing experimental data, obtained from a combination of point sources as well as a volumetric soil sample, to the simulated detector efficiencies. The average difference between the experimental and simulated FEP values was 2%, reported for a mixed gamma source. The highest reported discrepancy between experimental and simulated FEP values was 5% for the 59 keV peak of ^{241}Am. (Ješkovský et al., 2019) modelled a p-type HPGe detector (Canberra, model GC3020) with the Geant4 Monte Carlo code. Simulated FEP efficiencies were compared to experimentally determined FEP efficiencies for both a volumetric Marinelli geometry source and multiple point sources. In the range of 60 to 1800 keV, the model was not more than 5% different from the experimental values. However, at lower energies differences of 15% were reported for the 39.6 keV gamma ray of ^{129}I and for ^{152}Eu a difference of 8 to 9% was observed although no information was given on which gamma-ray emission was used to calculate the relative difference of ^{152}Eu.

Another frequently used Monte Carlo code is the MCNP5 code. (Chuong et al., 2016) estimated the inner dead-layer thickness of a n-type HPGe detector. Multiple point sources were measured experimentally at a distance of 5 and 10 cm from the detector endcap. The MCNP5 model showed an agreement within 3% of relative difference to the experimental values in an energy range of 88 to 1836 keV. (Salman et al., 2019) also used MCNP5 to study the FEP of a HPGe detector. In their research, the performance of the modelled ORTEC© HPGe (ORTEC© Model GEM100P4) detector was within 3% relative difference to the experimental values. (Saraiva et al., 2016) modelled an ORTEC GMX45 HPGe detector with MCNPX. Their model showed a 4% relative difference with experimental data, acquired by measuring a multi-gamma volume source placed at 4.54 mm and 26.12 mm from the endcap. However, a greater deviation of 6.5% was observed for the 46.5 keV gamma-ray peak of ^{210}Pb. Next to the aforementioned Monte Carlo codes, other codes have been used for simulating the detector response of HPGe detectors, such as PENELOPE, MCSHAPE etc. (G. Guerra et al., 2018)(Fernandez and Scot, 2009)

TOPAS, which stands for TOol for PArticle Simulation, is a Monte Carlo code that wraps and extends Geant4. The code is developed to be user friendly, as the user does not need to program the desired model in C++ code, as in Geant4. However, full accessibility to all Geant4 functionalities is still possible as custom extensions can be created, and compiled to extend TOPAS. Although the TOPAS MC code has been created initially for proton therapy and is used mainly within medical applications, it can also be used to study nuclear physics, particle physics, radiation damage and astrophysics (Perl et al., 2012)(Faddegon et al., 2020). However, in none of the aforementioned fields, TOPAS has been used or validated for gamma-ray spectrometry applications or detector calibrations. Nonetheless, the use of TOPAS in any of the aforementioned fields might be useful for checking the efficiency calibration of the radiation detectors with radioactive sources.

In this study, the use of TOPAS MC for gamma-ray spectrometry applications was investigated for coaxial p-type HPGe detector, model GX9023 from Canberra. TOPAS was used to model the HPGe detector and to study the performance of simulated efficiency calibrations of the detector directly to experimentally determined values.

2 MATERIALS AND METHODS

2.1 HPGE DETECTOR

The HPGe detector used for the experiments is named CAN03 and is located in the radionuclide metrology laboratory of the Joint Research Centre in Geel, Belgium. CAN03 is an extended range coaxial p-type germanium detector, from Canberra/Mirion. This detector has a reported relative efficiency of 90%. Its energy resolution is reported at 22, 88 and 1332 keV and is respectively 1.3, 1.4 and 2.3 keV full width at half maximum (FWHM). The detector has a useful energy range of 30 keV up to >10 MeV according to the manufacturer's specifications.

The detector layout comprises a copper endcap surrounding the detector internals, a crystal holder made out of copper with an inside sleeve of PTFE, and a 3x3 inch germanium crystal. The detector MC model is based on the technical drawings of the manufacturer. The dead layer values are transferred from an EGSnrc

model that is currently used at JRC which has already been validated using the same imposed criteria regarding the relative difference (see §2.4) as was used in this research. The used dead layer thicknesses in the MC model are listed in Table 1. Fig. 1 represents a visual representation of the of the MC detector model.

2.2 RADIOACTIVE SOURCES

Three different radionuclide geometries were used to determine the experimental efficiency of the coaxial detector. These radionuclide geometries are:

- Point source geometry (at 2 different heights);
- Volumetric water source (at 4 different heights);
- Volumetric silicone based source (at 2 different heights).

The point sources are from the Physikalisch-Technische Bundesanstalt (PTB) and have a certified activity. Only one radionuclide was present in each PTB source. A total of 5 different PTB point sources were measured having certified activities for respectively ^{137}Cs, ^{134}Cs, ^{60}Co, ^{152}Eu and ^{241}Am. The reference dates for the activity of these sources are respectively 01/01/2000, 01/10/2007, 01/12/2001, 01/01/2003 and 01/01/2000. The radionuclides were chosen to cover a wide range of photon energies, allowing for a comparison with the TOPAS MC results over a broad energy range. The PTB sources were placed at a precisely known position relative to the detector endcap with the help of low-density polyethylene (LDPE) spacers. Two different spacers were used to measure the PTB sources at 6.5 mm and 86.3 mm. The distances reported in this article are the distances between the highest point of the detector (copper part of the endcap) and the lowest point of the sources.

The volumetric water source will be referred to as the NPL source as this source was created at the National Physical Laboratory. The source was used in an environmental radioactivity proficiency test exercise in 2012 and consists of a PTFE cylindrical container, filled with water containing a radionuclide mix. The mixed radionuclides are ^{60}Co, ^{137}Cs, ^{134}Cs, ^{133}Ba and ^{152}Eu. For each of these radionuclides, the experimental efficiencies are calculated based on the NPL assigned values at reference date 01/10/2012. The NPL source was measured at 0.0 mm, 20.0 mm, 30.0 mm and 40.0 mm distance from the endcap.

The volumetric silicone based source was created at the Czech Metrology Institute and will be referred to as the CBSS2 source. This source consists of a PTFE cylindrical container, filled with a silicone resin with an elemental composition of 0.324 carbon, 0.081 hydrogen, 0.216 oxygen and 0.379 silicone (mass fractions). The silicone material is spiked with the radionuclides ^{139}Ce, ^{60}Co, ^{137}Cs, ^{113}Sn, ^{85}Sr, ^{57}Co, ^{51}Cr, ^{88}Y, ^{133}Ba, ^{109}Cd, ^{241}Am and ^{210}Pb. The CBSS2 source was measured at 0.0 mm and 40.0 mm distance from the endcap. The reference date for the source activity is 30/11/2018. Fig. 2 represents a technical drawing of the NPL source (top left), the CBSS2 source (top right) and the PTB source (bottom). The radionuclide activities that were used to calculate the experimental efficiency of the HPGe detector are listed in Table 2. The reported uncertainties are the combined standard uncertainty on the source activity, with a coverage factor of k=1.

2.3 MONTE CARLO MODEL

TOPAS version 3.5 was used for the simulations of the detector. The simulations were run on a CentOS7 Linux operating system. The geometry of the HPGe detector, as well as the used sources are based on the technical drawings of Fig. 1 and Fig. 2. For each source geometry, a set of two simulations was run for simulating respectively mono-energetic photons (with corresponding energies of the photons being emitted during the radioactive decay) and complete radioactive decays of the radionuclides. TOPAS uses Geant4 libraries for simulating full radioactive decays. The used nuclear data is from the Evaluated Nuclear Structure Data File (ENSDF) database. The first simulation results were used to determine the FEP peak efficiency of the Monte Carlo model ε_{MCp} per photon. The results of the decay simulations were used to calculate the FEP efficiency of the Monte Carlo model ε_{MCd} per decay. The following equations were used to calculate ε_{MCp} and ε_{MCd}:

$$\varepsilon_{MCp} = \frac{C_p}{H_p} \quad (1)$$

$$\varepsilon_{MCd} = \frac{C_d}{H_d} \quad (2)$$

Where C_p is the number of counts registered in the energy bin of the energy of interest as a result of photon simulations and H_p is the number of histories that were simulated which corresponds to the number of simulated photons. C_d is the number of counts registered in the energy bin of the energy of interest as a result of the decay simulations and H_d is the number of histories that were simulated which corresponds to the number of simulated decays. ε_{MCp} and ε_{MCd} are used to calculate a correction factor to account for true

coincidence summing. In the absence of summing effects $\varepsilon_{MCd}/\varepsilon_{MCp}$ equals the gamma-ray emission probability. For each decay simulation, 10x10^7 histories were run. For the photon simulations 10x10^7 histories were simulated. Only statistical uncertainties on ε_{MCp} and ε_{MCd} are taken into account.

The TOPAS model uses the standard physics list "g4em-standard_opt4"(Geant4, 2020), and a customised physics list named "tsradioactivedecay". The physics list specifies what physics processes and particles are used during the simulation. The customised physics list was created to have access to the Geant4 functionality of setting the command "nucleusLimit" which can be used to stop the radioactive decay process to the ground state of the first decay product. The different sources were simulated with the standard, built in volumetric source type provided by TOPAS which creates random starting positions for the generated particles within a user defined material. Simulations of the photons were started with the standard beam functionality with a beam kinetic energy of 0 MeV. The "energyspectrumvalue" was set to the energy corresponding to the desired photon energy (e.g. 1.33 MeV for the second gamma-ray emission of ^{60}Co) and the "beamparticle" was set to "gamma" to simulate photons. Simulations of the radioactive decays also used the standard "beam" functionality with a beam kinetic energy of 0 MeV but the "beamparticle" was of a "GenericIon" type (e.g. "GenericIon(27,60)" for simulating ^{60}Co). For the decay simulations, the "NucleusLimit" functionality provided by the customised physics list were set with commands for setting "MinimumZ", "MaximumZ", "MinimumA" and "MaximumA".

Results of the Monte Carlo simulations were scored with an energy deposit scorer. This scorer is set to the geometry component and an active material of interest, which was the active part of the germanium crystal consisting of the active material germanium. Energy deposit was scored in a histogram of 60x10^3 bins from 0 MeV up to 3 MeV, resulting in energy bins of each 0.05 keV in width. The output was an XML-format which was analysed and processed using Python.

2.4 EFFICIENCY CALIBRATION

Spectra were acquired and analysed with the Genie 2000 gamma-ray acquisition and analysis software. Data acquisition times were chosen to obtain adequate counts in the peak of interest to minimize statistical uncertainties to about 1%. The experimental FEP efficiency ε_{exp} was calculated for the most relevant photons of each radionuclide. The ε_{exp} was calculated with the following formula:

$$\varepsilon_{exp} = \frac{N_c}{A\ t\ P_\gamma} C_i \tag{3}$$

where N_c is the net number of counts in the region of interest (background and continuum corrected), A the activity of the source at the measurement time, t the live measurement time, P_γ the gamma-ray emission probability and C_i a correction factor for the dead time, radioactive decay during the measurement and true coincidence summing events. Since the live measurement time already includes a dead-time correction, no further corrections were made to correct for dead-time count losses in C_i. Furthermore, no decay correction was applied as the measurement times were short compared to the half-life of the measured radionuclides. As a result, C_i only includes a correction for the true coincidence summing events and was determined with the following formula:

$$C_i = \frac{\varepsilon_{MCp}}{\varepsilon_{MCd}/P_\gamma} \tag{4}$$

Where ε_{MCp} is the FEP efficiency determined by the TOPAS MC model when simulating mono-energetic photons, P_γ the gamma-ray emission probability and ε_{MCd} the FEP efficiency determined by the TOPAS MC model when simulating decays. As ε_{exp} includes a coincidence correction factor which is derived from the MC simulations, it should not be interpreted as a completely experimental FEP efficiency. The uncertainty of ε_{exp} was determined with the following equation (Lépy et al., 2017):

$$\frac{s_{\varepsilon_{exp}}}{\varepsilon_{exp}} = \sqrt{\left(\frac{s_{Nc}}{N_c}\right)^2 + \left(\frac{s_A}{A}\right)^2 + \left(\frac{s_t}{t}\right)^2 + \left(\frac{s_{\varepsilon_{MCp}}}{\varepsilon_{MCp}}\right)^2 + \left(\frac{s_{\varepsilon_{MCd}}}{\varepsilon_{MCd}}\right)^2} \tag{5}$$

Where the numerator of each term represents the uncertainty on respectively the background and continuum corrected net area of the peak of interest (s_{Nc}), the activity (s_A), the live time (s_t), the FEP efficiency determined by the TOPAS MC model when simulating mono-energetic photons (s_{eMCp}) and the FEP efficiency determined by the TOPAS MC model when simulating decays (s_{eMCd}).

In a next step, the calculated values for ε_{exp} of each energy of interest were used for a least-squares fit to obtain an efficiency equation covering the energy range from the lowest measured energy to the highest measured energy. The energy efficiency was fitted to a polynomial of the fourth order:

$$\log(\varepsilon_{\exp}) = a_0 + a_1 \log\left(\frac{C}{E_\gamma}\right) + a_2 \log\left(\frac{C}{E_\gamma}\right)^2 + a_3 \log\left(\frac{C}{E_\gamma}\right)^3 + a_4 \log\left(\frac{C}{E_\gamma}\right)^4 \quad (6)$$

where a_0 to a_4 were the fitting parameters determined by the least-square method and C was determined following the equation:

$$C = \ln\left(\frac{E_{max}+E_{min}}{2}\right) \quad (7)$$

Parameters E_{min} and E_{max} are respectively the minimum and maximum photon energy within the source that was used to define the energy efficiency equation.

2.5 VALIDATING THE MODEL

To validate the Monte Carlo model, the experimental FEP efficiency $\varepsilon_{\exp}$ was compared to the FEP efficiency of the Monte Carlo model $\varepsilon_{\mathrm{MCp}}$. For each energy of interest, the relative difference in percentage between $\varepsilon_{\exp}$ and $\varepsilon_{\mathrm{MCp}}$ was determined with equation:

$$D_r = \left(\frac{\varepsilon_{\exp}}{\varepsilon_{\mathrm{MCp}}} - 1\right) 100 \quad (8)$$

In a second step, the performance of the efficiency equation was compared to $\varepsilon_{\exp}$ by calculating the relative residuals. The relative residuals, expressed as a percentage, are determined with equation:

$$R_r = \left(\frac{\varepsilon_{\mathrm{fit}}}{\varepsilon_{\exp}} - 1\right) 100 \quad (9)$$

The performance of the Monte Carlo model was compared to an imposed criteria of 5% relative difference for gamma rays with an energy of between 100 keV and 2000 keV and 10% relative difference for gamma rays with energies lower than 100 keV or higher than 2000 keV. The measurement time of the different sources was chosen to yield counting statistics of about 1% for the most predominant gamma-ray energies of the chosen radionuclides.

3 RESULTS AND DISCUSSION

3.1 POINT SOURCES

PTB point sources were measured at a height of 6.5 mm and 86.3 mm from the centre of the detector endcap. Five different PTB sources, containing respectively ^{137}Cs, ^{134}Cs, ^{60}Co, ^{152}Eu and ^{241}Am, were measured. Fig. 3 shows a full plot of both the experimental and simulated spectrum of ^{137}Cs measured at 6.5 mm from the detector endcap. For this comparison, the energy bin width of the TOPAS model was set to match the bin width of the data acquisition system. As can be observed, the datasets show good agreement for not only the FEP but also for the X-ray emission peaks and the shape of the Compton continuum. It should however be mentioned that one should always be careful when comparing spectral data of a Monte Carlo simulation directly to an experimental spectrum as the resolution of a HPGe detector system depends on electronic noise of the whole electronic chain. This noise is not included in Monte Carlo models which only describe particle and photon interactions.

In Fig.4, the comparison of the FEP efficiency of the simulated and experimental values are plotted. The experimental spectra were analysed with Genie2000 software and the interactive peak fit function. The experimental counts for each energy were then used in equation 3 to yield the experimental FEP efficiency of the detector. The experimental data points are plotted in colour, each colour represents a different source-to-endcap distance. Data points of the MC simulations are plotted with black crosses. The uncertainties on the data points were calculated with equation 5 for the experimental data points. For the simulated efficiencies, the reported uncertainty is given by the statistical uncertainty of the Monte Carlo simulation. The relative uncertainties on the experimental data range from 0.53% for the 604 keV gamma-ray energy of ^{134}Cs (measured at 86.3 mm) up to 2.72% for the 688 keV gamma-ray energy of ^{152}Eu (measured at the detector endcap). A least-square fit on the experimental data points was also carried out to determine the detector efficiency curve as described by equation 6. The resulting efficiency calibration equation is plotted in black in the top graph of Fig. 4.

The relative differences, calculated by equation 8 are plotted in the middle of Fig. 4. Over the entire range of simulated energies, the relative differences are smaller than the imposed acceptable limits of 5% in the energy range of 100 keV to 2000 keV and 10% relative difference in the energy range below 100 keV or above 2000 keV. The highest relative difference is 4.66%. This is again linked to the 688.67 keV gamma-ray energy of ^{152}Eu (measured at the detector endcap). The lowest relative difference was observed for the 661 keV gamma-ray energy of ^{137}Cs at 0.23%. When comparing the relative differences of the two different

heights, the overall performance of the measurements at 86.3 mm are in better agreement with the experimental data compared to the measurements at endcap. This is an expected result, as small differences in source to detector geometries are more critical close to the detector endcap compared to larger source to detector distances.

The final comparison of the PTB point sources results are the relative residuals calculated according to equation 9 and plotted in the bottom graph of Fig. 4. The residuals assess the performance of the least-square fit on the experimental data and compare the fit to the experimental data points. For both source-to-detector distances, the fitted polynomial fits the data well, as the relative residuals are within a 4% margin. The overall better performance of the measurement at 86.3 mm is again visible, as the relative residuals vary less over the entire energy range compared to the measurements directly at the endcap.

3.2 VOLUMETRIC WATER SOURCE

The volumetric water source contained ^{60}Co, ^{137}Cs, ^{134}Cs, ^{133}Ba and ^{152}Eu. The specific activities were based on the assigned activity value obtained by the results of the proficiency test carried out in 2012. Both the experimental data and the MC results are shown in Fig. 5 for distances of 0 mm, 20 mm, 30 mm and 40 mm of distance from the endcap. The simulated detector efficiencies are plotted in black crosses whereas the experimentally determined detector efficiencies are plotted in colour. The relative uncertainties of the experimental data range from 0.19% for the 1332 keV gamma-ray energy of ^{60}Co (measured at the endcap) up to 2.34% for the 801 keV gamma-ray energy of ^{134}Cs (measured at 20 mm). As for the point sources, the results of the volumetric water source are in agreement with the imposed criteria for the relative difference. The lowest relative difference was 0.02% for the 801.95 keV gamma-ray energy of ^{134}Cs (at 20 mm). Only for the 688.67 keV gamma-ray energy of ^{152}Eu this criteria was not achieved as a slightly higher relative difference of 5.12% was observed for the measurement at 20 mm endcap distance. As for the measurements of the PTB source, the slightly elevated relative difference for this gamma-ray energy can be explained by the small P_γ and the interference of the 686.61 keV gamma-ray emission of ^{152}Eu.

The relative residuals are plotted in the bottom graph of Fig. 5. The relative residuals range between 0.06% relative difference (for the 661.66 keV peak of ^{137}Cs at 40 mm) and -4.27% relative difference (for the 688.67 keV peak of ^{133}Ba at 20 mm) indicating a correct fit of the fourth order polynomial to the experimental data.

3.3 VOLUMETRIC SILICONE SOURCE

The volumetric silicone source contained radionuclides ^{139}Ce, ^{60}Co, ^{137}Cs, ^{113}Sn, ^{85}Sr, ^{57}Co, ^{51}Cr, ^{88}Y, ^{133}Ba, ^{109}Cd, ^{241}Am and ^{210}Pb. The top graph of Fig. 6 shows the results for the simulated and experimental detector efficiency of the CBSS2 source, measured at two different heights (0 mm and 40 mm distance from the detector endcap). The experimental efficiency data points are plotted in colour representing the values for 0 mm and 40 mm. the simulated efficiencies for both geometries are plotted in black. The relative uncertainties on the experimental efficiencies were of the order of 1% and depend on the counting statistics of the peaks of interest. Only for the 2734.09 keV peak of ^{88}Y, which showed the highest experimental uncertainty at 4.47% and 6.02% for respectively 0 mm and 40 mm, this criteria was not met. This is a result of the low counting statistics related to this peak due to the low P_γ of 0.608% of this gamma-ray emission. The same observation for the 2734.09 keV peak of ^{88}Y can also be made when looking at the relative differences, plotted in the centre of Fig. 6 as this peak shows the biggest relative difference of 4.88% at 0 mm. As with the other measured geometries, the overall performance of the MC model improves when larger source to endcap distances are used. Again referring to the 2734.09 keV peak of ^{88}Y, this is illustrated by the lower relative difference of -1.79% observed when a source to endcap distance of 40mm is used. Irrespective of the source to endcap distance, all calculated relative differences for the twelve radionuclides in the CBSS2 source respected the imposed acceptance interval. The fourth order polynomial also provided an adequate fit for the efficiency of the CBSS2 source. For both the 0 mm and 40 mm geometries the fit shows good agreement with the experimental data. The relative residuals for the 0 mm geometry vary between 4.23% (661.66 keV) and -4.12% (688.70 keV).

4 CONCLUSIONS

The current study demonstrates the use of TOPAS MC for gamma-ray spectrometry applications by comparing experimental data with simulated FEP efficiencies of a HPGe detector. The TOPAS MC model was examined for three different radionuclide geometries, each of which was measured at different detector to endcap distances:

- Point source geometry (at 2 different heights): different sources were used which contained respectively ^{137}Cs, ^{134}Cs, ^{60}Co, ^{152}Eu and ^{241}Am;
- Volumetric water source (at 4 different heights): this source was part of a proficiency test and contained ^{60}Co, ^{137}Cs, ^{134}Cs, ^{133}Ba and ^{152}Eu;
- Volumetric silicone source (at 2 different heights): this reference source contained ^{139}Ce, ^{60}Co, ^{137}Cs, ^{113}Sn, ^{85}Sr, ^{57}Co, ^{51}Cr, ^{88}Y, ^{133}Ba, ^{109}Cd, ^{241}Am and ^{210}Pb.

The performance of the Monte Carlo model was compared to an imposed criteria of 5% relative difference for gamma rays with an energy of between 100 keV and 2000 keV and 10% relative difference for gamma rays with energies lower than 100 keV or higher than 2000 keV. The TOPAS MC model was in good agreement with the imposed criteria for each of the examined radionuclide geometries. A small deviation from this criteria was however observed for the 688.67 keV gamma-ray energy of ^{152}Eu for the measurement of the volumetric water source at 20 mm endcap distance. This is, however, not due to errors in the MC model, but is linked to the experimental error due to the small P_γ and the interference of the 686.61 keV gamma-ray emission of ^{152}Eu. As a result, the use of TOPAS MC for gamma-ray spectrometry applications as well as the constructed MC model of the Canberra coaxial detector can be considered validated.

5 ACKNOWLEDGMENTS

The research was conducted under a PhD grant at Hasselt University. This work received support from the open access scheme EUFRAT at the European Commission's Joint Research Centre in Geel. The author would also like to thank the developer team of TOPAS MC for the special licence allowing the use of TOPAS MC for gamma-ray spectrometry applications.

6 REFERENCES

Cebastien Joel, G.S., Maurice, N.M., Eric Jilbert, N.M., Ousmanou, M., David, S., 2018. Monte Carlo method for gamma spectrometry based on GEANT4 toolkit: Efficiency calibration of BE6530 detector. J. Environ. Radioact. 189, 109–119. https://doi.org/10.1016/j.jenvrad.2018.03.015

Chuong, H.D., Thanh, T.T., Ngoc Trang, L.T., Nguyen, V.H., Tao, C. Van, 2016. Estimating thickness of the inner dead-layer of n-type HPGe detector. Appl. Radiat. Isot. 116, 174–177. https://doi.org/10.1016/j.apradiso.2016.08.010

Croymans, T., Schroeyers, W., Krivenko, P., Kovalchuk, O., Pasko, A., Hult, M., Marissens, G., Lutter, G., Schreurs, S., 2017. Radiological characterization and evaluation of high volume bauxite residue alkali activated concretes. J. Environ. Radioact. 168, 21–29. https://doi.org/10.1016/j.jenvrad.2016.08.013

Faddegon, B., Ramos-Méndez, J., Schuemann, J., McNamara, A., Shin, J., Perl, J., Paganetti, H., 2020. The TOPAS tool for particle simulation, a Monte Carlo simulation tool for physics, biology and clinical research. Phys. Medica 72, 114–121. https://doi.org/10.1016/j.ejmp.2020.03.019

Fernandez, J.E., Scot, V., 2009. Simulation of the detector response function with the code MCSHAPE. Radiat. Phys. Chem. 78, 882–887. https://doi.org/10.1016/j.radphyschem.2009.04.018

G. Guerra, J., G. Rubiano, J., Winter, G., G. Guerra, A., Alonso, H., Arnedo, M.A., Tejera, A., Mosqueda, F., Martel, P., Bolivar, J.P., 2018. Automatic modeling using PENELOPE of two HPGe detectors used for measurement of environmental samples by γ-spectrometry from a few sets of experimental efficiencies. Nucl. Instruments Methods Phys. Res. Sect. A Accel. Spectrometers, Detect. Assoc. Equip. https://doi.org/10.1016/j.nima.2017.10.076

Geant4, 2020. Physics reference manual - Release 10.6 Rev4.1, 1–558.

Hult, M., Geelen, S., Stals, M., Lutter, G., Marissens, G., Stroh, H., Schreurs, S., Schroeyers, W., Bruggeman, M., Verheyen, L., 2019. Determination of homogeneity of the top surface deadlayer in an old HPGe detector. Appl. Radiat. Isot. 147, 182–188. https://doi.org/10.1016/j.apradiso.2019.02.019

Hult, M., Marissens, G., Stroh, H., Lutter, G., Tzika, F., Marković, N., 2018. Characterisation of an ultra low-background point contact HPGe well-detector for an underground laboratory. Appl. Radiat. Isot. 134, 446–449. https://doi.org/10.1016/j.apradiso.2017.08.002

Ješkovský, M., Javorník, A., Breier, R., Slučiak, J., Povinec, P.P., 2019. Experimental and Monte Carlo determination of HPGe detector efficiency. J. Radioanal. Nucl. Chem. 322, 1863–1869. https://doi.org/10.1007/s10967-019-06856-4

Khan, W., Zhang, Q., He, C., Saleh, M., 2018. Monte Carlo simulation of the full energy peak efficiency of an HPGe detector. Appl. Radiat. Isot. 131, 67–70. https://doi.org/10.1016/j.apradiso.2017.11.018

Lépy, M.C., Pearce, A., Sima, O., 2017. Corrigendum : Uncertainties in gamma-ray Corrigendum : Uncertainties in gamma-ray.

Lutter, G., Hult, M., Marissens, G., Stroh, H., Tzika, F., 2018. A gamma-ray spectrometry analysis software environment. Appl. Radiat. Isot. 134, 200–204. https://doi.org/10.1016/j.apradiso.2017.06.045

Perl, J., Shin, J., Schümann, J., Faddegon, B., Paganetti, H., 2012. TOPAS: An innovative proton Monte Carlo platform for research and clinical applications. Med. Phys. 39, 6818–6837. https://doi.org/10.1118/1.4758060

Salman, A., Ahmed, Z., Allam, K.A., El-Sharkawy, S., 2019. Investigation hybrid MCNP/Angle model for calculating the absolute full-energy peak efficiency of HPGe detector. Appl. Radiat. Isot. 150, 57–62. https://doi.org/10.1016/j.apradiso.2019.04.030

Saraiva, A., Oliveira, C., Reis, M., Portugal, L., Paiva, I., Cruz, C., 2016. Study of the response of an ORTEC GMX45 HPGe detector with a multi-radionuclide volume source using Monte Carlo simulations. Appl. Radiat. Isot. 113, 47–52. https://doi.org/10.1016/j.apradiso.2016.04.016

7 FIGURE CAPTIONS

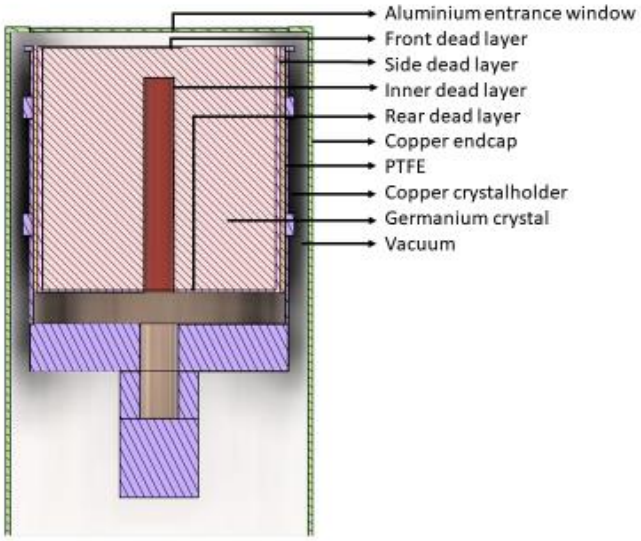

Figure 1: technical drawing of the CAN03 MC model.

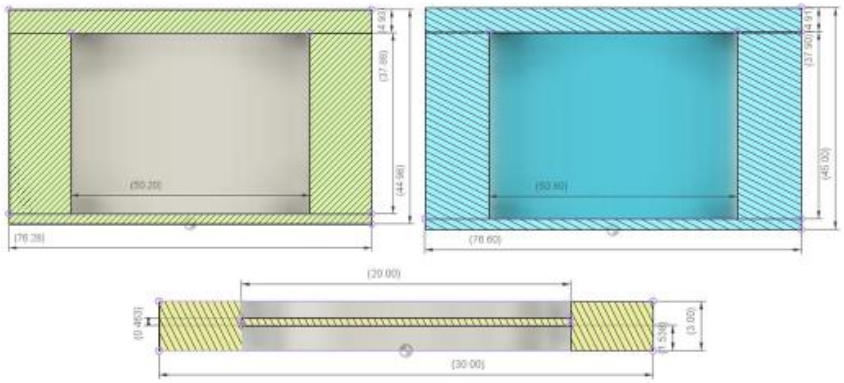

Figure 2: technical drawing of the cross-sections of the NPL source (top left), the CBSS2 source (top right) and the PTB source (bottom). All the used sources have a cylindrical shape. For the NPL and CBSS2 source the container material is PTFE. For the PTB source, the source material is LDPE. Dimensions are expressed in mm.

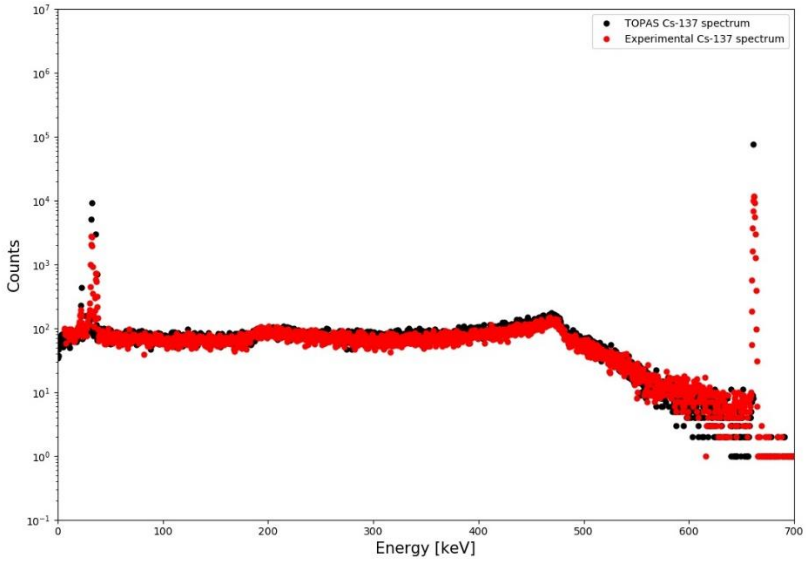

Figure 3: simulated and experimental spectrum of Cs-137 measured at 6.5 mm from the detector endcap.

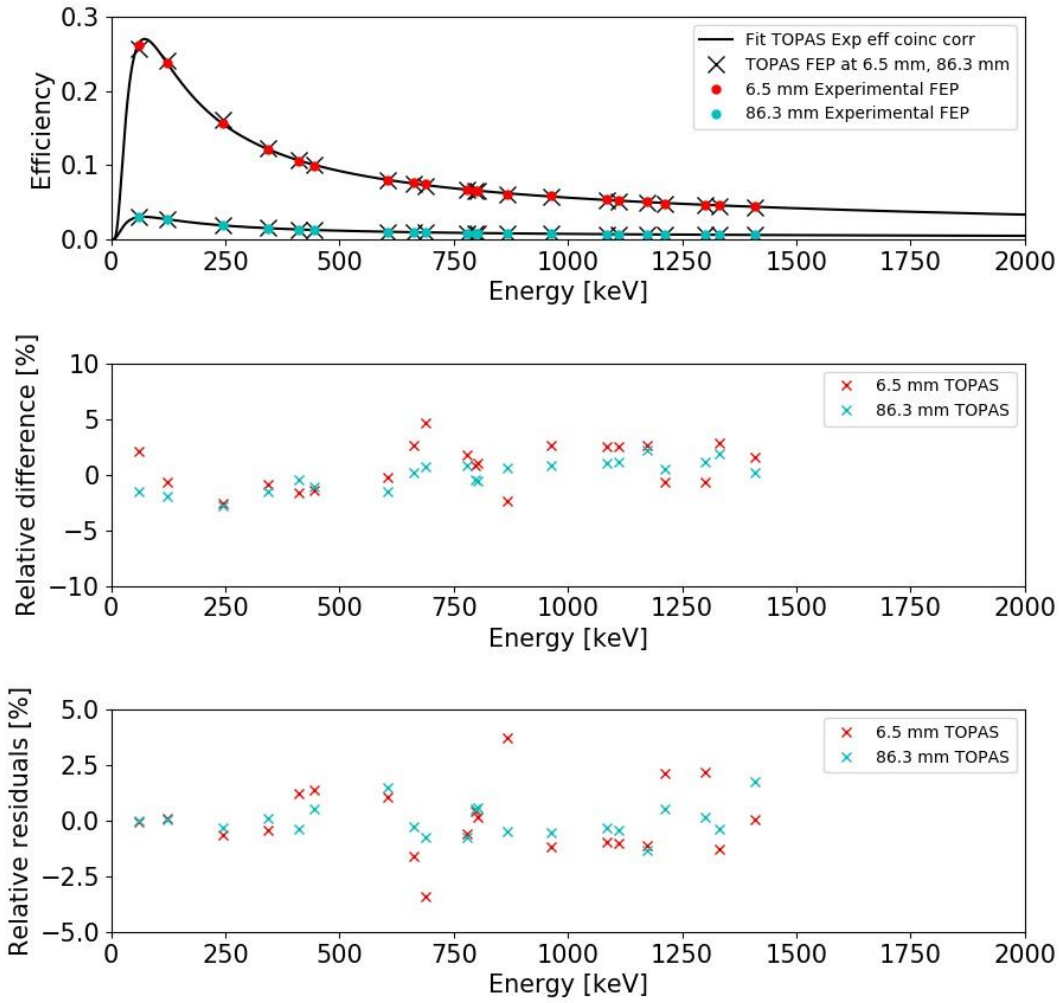

Figure 4: experimental and MC calculated detector efficiencies for measurements of the PTB point sources at 6.5 mm and 86.3 mm from the detector endcap (top). Relative difference between the experimental and MC detector efficiencies (middle). Relative residuals between the fitted efficiency calibration curve on the experimental data points and the experimental data points (bottom).

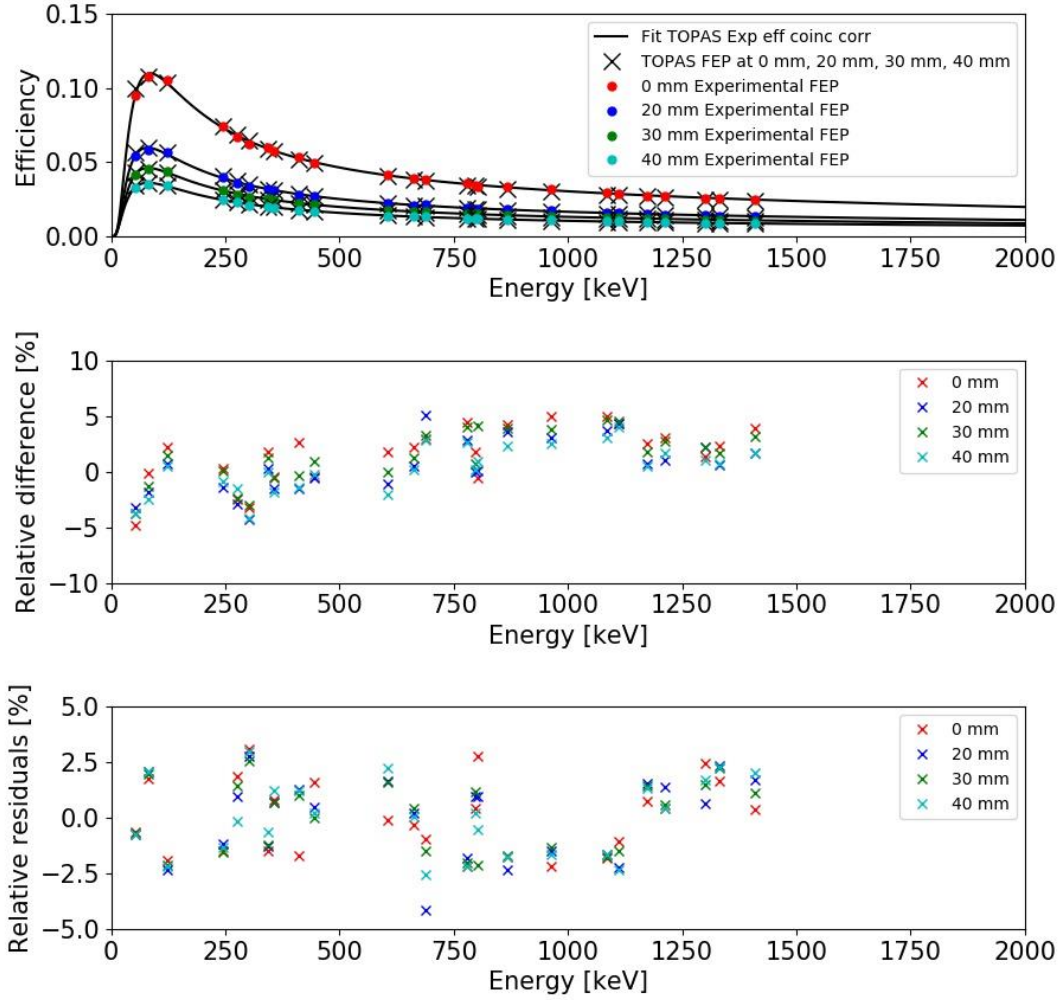

Figure 5: experimental and MC calculated detector efficiencies for measurements of the NPL source at 0 mm, 20 mm, 30 mm and 40 mm from the detector endcap (top). Relative difference between the experimental and MC detector efficiencies (middle). Relative residuals between the fitted efficiency calibration curve on the experimental data points and the experimental data points (bottom).

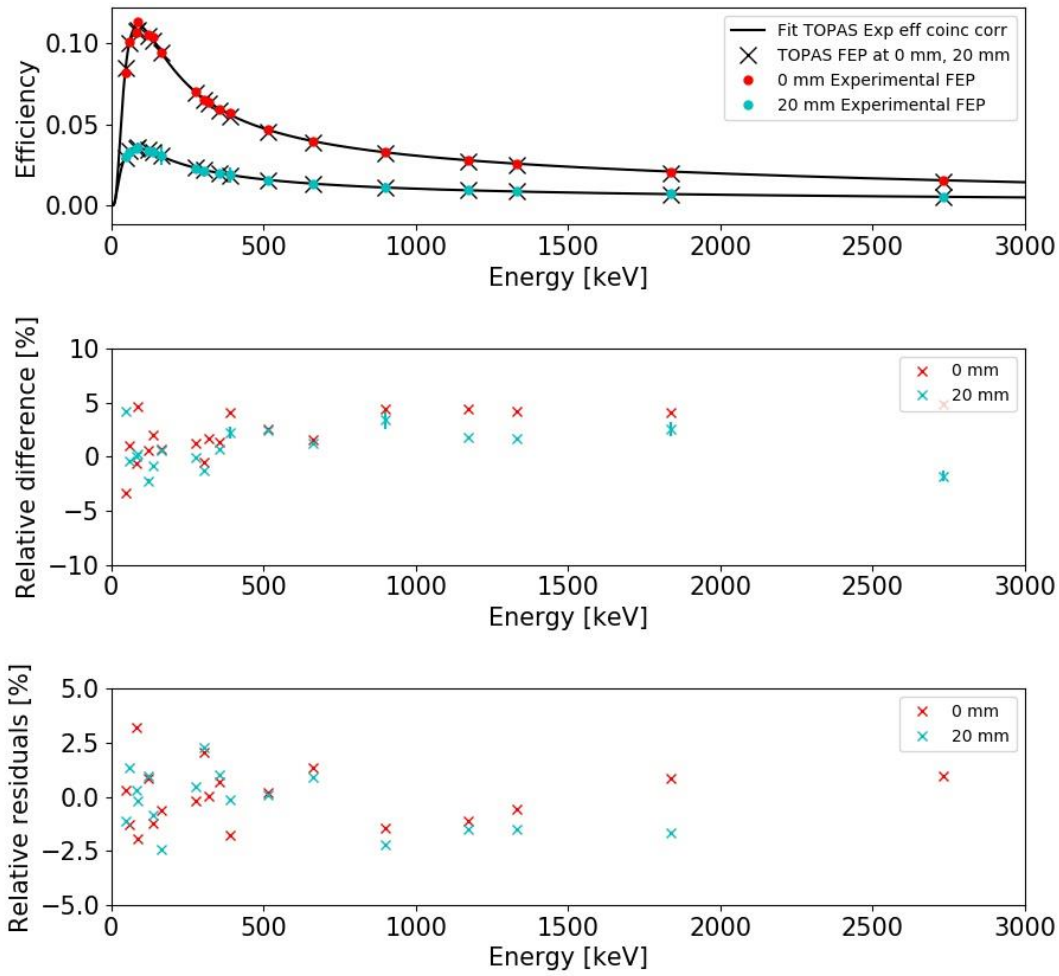

Figure 6: experimental and MC calculated detector efficiencies for measurements of the CBSS2 source at 0 mm and 40 mm from the detector endcap (top). Relative difference between the experimental and MC detector efficiencies (middle). Relative residuals between the fitted efficiency calibration curve on the experimental data points and the experimental data points (bottom).

8 TABLES

Table 1: dead layer thicknesses used in the MC model

Detector parameter	TOPAS MC input
Dead layer	
Front dead layer	0.4 µm
Side dead layer	1.5 mm
Inner dead layer	0.6 µm
Rear dead layer	0.7 mm

Table 2: source activities and their combined relative standard uncertainty on the source activity, at k=1

	PTB activity (kBq)	Unc. (%)	Ref. Date	NPL activity (kBq)	Unc. (%)	Ref. Date	CBSS2 activity (kBq)	Unc. (%)	Ref. Date
^{241}Am	11.71	0.5	1/01/2000	-	-	-	4.772	1.1	30/11/2018
^{133}Ba	-	-	-	0.5954	0.7	1/10/2012	1.696	1.2	30/11/2018
^{109}Cd	-	-	-	-	-	-	14.69	1.5	30/11/2018
^{139}Ce	-	-	-	-	-	-	0.8159	1.7	30/11/2018
^{57}Co	-	-	-	-	-	-	0.8308	1.9	30/11/2018
^{60}Co	9.92	0.4	1/12/2001	0.4202	0.2	1/10/2012	2.623	1.1	30/11/2018
^{51}Cr	-	-	-	-	-	-	20.10	1.7	30/11/2018
^{134}Cs	11.70	0.4	1/10/2007	0.2250	0.7	1/10/2012	-	-	-
^{137}Cs	6.46	0.5	1/01/2000	1.238	0.4	1/10/2012	2.342	1.2	30/11/2018
^{152}Eu	4.28	0.7	1/01/2003	1.226	0.7	1/10/2012	-	-	-
^{210}Pb	-	-	-	-	-	-	19.23	1.5	30/11/2018
^{113}Sn	-	-	-	-	-	-	3.241	1.3	30/11/2018
^{85}Sr	-	-	-	-	-	-	3.838	1.5	30/11/2018
^{88}Y	-	-	-	-	-	-	6.57	1.1	30/11/2018